ELSEVIER

Journal of Molecular Catalysis A: Chemical 122 (1997) 81–90

JOURNAL OF MOLECULAR CATALYSIS A: CHEMICAL

Investigations on the aqueous solution and solid-state cation exchanged MAPO-ATS type molecular sieve

Deepak B. Akolekar *, Suresh Bhargava

Applied Chemistry Department, Royal Melbourne Institute of Technology, City Campus, Melbourne, Vic. 3001, Australia

Received 4 September 1996; accepted 17 December 1996

Abstract

MAPO-36 (magnesium substituted aluminophosphate of ATS type) have been prepared and modified by the liquid mediated cation exchange and contact induced cation exchange methods. Modified samples prepared by the liquid cation exchange (sodium/caesium/calcium-MAPO-36) and solid-state ion exchange at different temperatures (sodium-MAPO-36) were studied by XRD, SEM, FTIR, TG, BET, ^{27}Al and ^{31}P MAS NMR. The XRD, SEM and FTIR results indicate that the crystal structure and crystal morphology of Na/Cs/Ca exchanged MAPO-36 samples prepared by liquid cation exchange method are similar to the parent calcined MAPO-36 material. However, the crystal phase morphology and surface area are drastically affected when the sodium exchanged MAPO-36 samples are prepared by the solid-state reaction. Above 723 K and in the presence of sodium chloride, a dense tridymite phase formation from the ATS phase was observed. ^{27}Al MAS NMR spectra of the Na/Cs/Ca MAPO-36 samples prepared by liquid cation exchange are similar to that of MAPO-36 and show characteristic peaks for tetrahedral and pentahedral coordinated Al. In the contact induced cation exchanged samples, symmetric and narrow ^{27}Al NMR peak related to tetrahedrally coordinated Al was observed. The ^{31}P MAS NMR of the MAPO-36 and the samples prepared by liquid cation exchange are similar but differ significantly from those samples prepared by solid-state cation exchange. The catalytic activity of the MAPO-36 and the sodium exchanged samples prepared by liquid and solid-state cation exchanges in the *o*-xylene conversion reaction was studied.

Keywords: MeAPO; Aluminophosphate molecular sieve; MAPO-36; Cation exchange; Solid-state cation exchange; ^{27}Al and ^{31}P MAS NMR

1. Introduction

New materials like metal incorporated aluminophosphates (MeAPO-n) reported by Flanigen et al. [1,2] are of growing interests. It is well known that the properties of aluminophosphate molecular sieve catalysts [3,4] can be altered by isomorphous substitution of various elements for Al/P in the aluminophosphate framework. There are other catalyst modification methods (such as thermal, hydrothermal, acid and base treatments and ion exchange method) which influence the catalytic as well as other properties of zeolitic materials. The most commonly used methods are the ion exchange mediated by a liquid phase and by solid-state ion exchange in zeolites [5–9]. Karge and coworkers have systematically studied the solid-state ion exchange in zeolites viz. alkaline chlorides-ZSM-5 [10] and metal chlorides-NaY systems [11]. They have observed that mixtures of solid alkaline chlorides and NH_4-ZSM-5/H-

* Corresponding author.

PII S1381-1169(97)00015-0

ZSM-5 react at elevated temperatures to form cationic ZSM-5.

In MeAPO-n materials, the framework negative charge is balanced by proton or cation, which leads to generation of Brønsted acidity/ion exchange capacity. Modification of the MeAPOs by ion exchanges are less studied. Current work was undertaken with an objective of exploring the properties of metal aluminophosphate affected by liquid phase ion exchange and solid-state ion exchange. In the present investigation, cation exchanged MAPO-36 samples prepared by aqueous solution ion-exchange and solid-state ion exchange methods are examined by X-ray diffractometry, SEM, FTIR, thermal analysis, BET, ^{27}Al and ^{31}P MAS NMR techniques.

2. Experimental

MAPO-36 molecular sieve was synthesised by the hydrothermal crystallization of a precursor-metal aluminophosphate gel. The gel composition and synthesis conditions utilized for the preparation of MAPO-36 are as follows: 1.85 Pr_3N, 0.17 MgO, 0.92 Al_2O_3, 1.02 P_2O_5, 40.0 H_2O; 378 K, 50 h and 423 K, 24 h. A uniform homogenous gel is prepared by mixing Al and P sources and water and then Mg source is added followed by the organic template. The source of Al_2O_3 was the psuedo-boehmite (courtesy Condea Vista Singapore, Inc.). The ortho-phosphoric acid [(90%) Merck] and magnesium acetate were used as a sources of P_2O_5 and MgO. The tri-n-propylamine used was synthetic grade supplied by Aldrich. The crystals of the magnesium aluminophosphate were washed thoroughly with deionized distilled water, filtered, and dried in an air oven at 373 K for 16 h. The organic template (tri-n-propylamine) was removed by calcination in the presence of air (flow rate 100 $cm^3 \cdot min^{-1}$) at 823 K for 20 h. The preparation and characterization of MAPO-36 used in the present study is given elsewhere [12].

The cation-exchange of MAPO-36 was carried out as follows: (i) *Liquid mediated cation-exchanged MAPO-36 samples*: NaMAPO-36(L), CsMAPO-36(L) and CaMAPO-36(L) samples were prepared by exchanging the calcined MAPO-36 (5.0 g) with 0.6 M NaCl aqueous solution [2500 cm^3] at 343 K for 24 h, 0.05 M CsCl solution [700 cm^3] at 350 K for 20 h (procedure repeated twice for Cs exchange) and 0.3 M CaCl solution [2500 cm^3] at 348 K for 24 h, respectively. The cation exchanged MAPO-36 samples were washed thoroughly with deionised water, filtered and dried in an vacuum oven at 373 K for 12 h and calcined at 773 K for 8 h. (ii) Solid-state cation exchanged MAPO-36 samples: NaMAPO-36(S1), NaMAPO-36(S2) and NaMAPO-36(S3) were prepared by dry grinding the mixtures of NaCl and MAPO-36 in an agate mortar and heat treating at 723 K for 20 h, 823 K for 20 h and 900 K for 10 h, respectively. Usually 3 g of MAPO-36 is mixed with 0.16 g of NaCl.

The details of characterisation techniques and instrument utilized for the chemical analysis and structure determination are reported earlier [12]. The surface area and pore volume of the materials were obtained by N_2-dynamic adsorption/desorption technique ($p/p_o = 0.3$) using a Micromeritics Instrument (ASAP2000) [Micromeritics Instrument Corporation, USA]. Perkin-Elmer [TGA7 series] thermal analyser was used to determine the amount of water sorbed in the materials. The morphology and crystal size of the materials were investigated using a JEOL JSM 35 MF scanning electron microscope. Infrared spectra of the samples in the lattice vibration region were obtained from KBr disks (1.2 wt.-%) at 2 cm^{-1} resolution using a Perkin-Elmer FTIR 1725X spectrometer.

NMR measurements were carried out using a Bruker MSL 300 spectrometer. NMR resonance frequencies were 78.188 MHz for ^{27}Al and 121.44 MHz for ^{31}P. Samples were spun in 4 mm (o.d) zirconia rotor at speed of 10 kHz. High power proton decoupling measurements

employed pulse widths of 15° and 25° and recycle times of 2 and 20 s for ^{27}Al and ^{31}P, respectively. Proton cross polarization ^{31}P measurements used a contact time of 5 milliseconds and a recycle time of 5 seconds. Chemical shifts were referenced to external kaolin (^{27}Al, $\delta = -2.5$ ppm) (for ^{27}Al) and ammonium dihydrogen phosphate (^{31}P, $\delta = 1$ ppm) (for ^{31}P).

The catalytic activity of the MAPO-36, NaMAPO-36[L], NaMAPO-36[S1], NaMAPO-36[S2] and NaMAPO-36[S3] in the *o*-xylene conversion reaction have been determined in a pulse microreactor (i.d. 4 mm) connected to a gas chromatograph. The reaction conditions are as follows: amount of catalyst, 0.050 g; N_2 – flow rate 125 $cm^3 \cdot min^{-1}$; pulse size 5 μl and temperature 673 K. Before the activity was measured, the catalyst was heated at 673 K for 1 h in a flow of nitrogen. The details of the microreactor, the experimental procedures for measuring the catalytic activity of the catalysts were reported earlier [13].

3. Results and discussion

For the cation exchange studies, highly crystalline MAPO-36 was obtained using the gel and synthesis conditions mentioned in the experimental section. The characteristics of MAPO-36 and cation exchanged MAPO-36 samples are presented in Table 1. The crystallinity, pore volume, surface area and SEM examination revealed the sample purity. The calcined MAPO-36 was used for preparing the liquid mediated and contact induced cation exchange samples.

The XRD patterns for MAPO-36, NaMAPO-36[L], NaMAPO-36[S1], NaMAPO-36[S2] and NaMAPO-36[S3] are shown in Fig. 1. The structure of the MAPO-36 remains the same after calcination at 823 K. NaMAPO-36[L] prepared from liquid cation exchange method do not indicate any changes in the structure, crystalline phase and crystallinity (Fig. 1b, Table 1). The changes are observed in the X-ray diffractograms of MAPO-36 samples prepared from contact induced cation exchanges at 723 K, 823 K and 900 K. The sample (NaMAPO-36[S1]) prepared by solid-state exchange at 723 K shows the presence of different phases (ATS and tridymite) with tridymite as a major phase and the ATS phase is around 11% (Fig. 1c). The heat treatment of the mixture of NaCl and MAPO-36 at higher temperatures (> 723 K) show complete transformation of the ATS phase to tridymite (Fig. 1d,e). Fig. 2 shows the CsMAPO-36[L] (Fig. 2b) and CaMAPO-36[L] (Fig. 2c) samples prepared from the liquid cation exchange method. Here, no changes are observed in the phase and crystallinity.

Fig. 3 shows the scanning electron micro-

Table 1
Data on the ATS magnesium aluminophosphate based materials

Material	Molar chemical composition	Crystallinity (100%)	Crystalline phase	Pore volume ($cm^3\ g^{-1}$)	External surface area ($m^2 g^{-1}$)	Total surface area ($m^2\ g^{-1}$)
MAPO-36	0.16 Mg 0.92 Al_2O_3 1.0 P_2O_5	100	ATS	0.173	36	475
NaMAPO-36[L]	0.082 Na 0.16 Mg 0.92 Al_2O_3 1.0 P_2O_5	100	ATS	0.081	42.0	207
NaMAPO-36[S1]	0.14 Na 0.16 Mg 0.92 Al_2O_3 1.0P_2O_5	89 T	ATS, T	0.008	25.6	29
NaMAPO-36[S2]	0.14 Na 0.16 Mg 0.92 Al_2O_3 1.0 P_2O_5	100 T	T	–	8.8	8.8
NaMAPO-36[S3]	0.14 Na 0.16 Mg 0.92 Al_2O_3 1.0 P_2O_5	100 T	T	–	7.6	7.6
CsMAPO-36[L]	0.07 Cs 0.16 Mg 0.92 Al_2O_3 1.0 P_2O_5	100	ATS	0.077	38	193
CaMAPO-36[L]	0.038 Ca 0.16 Mg 0.92 Al_2O_3 1.0 P_2O_5	100	ATS	0.084	39	222

L: liquid cation exchange at 353 K for 20 h, 1 M NaCl/CsCl/$CaCl_2$.
S1: solid-state exchange at 723 K for 16 h, nitrogen flow rate 70 $cm^3 \cdot min^{-1}$.
S2: solid-state exchange at 823 K for 16 h, nitrogen flow rate 70 $cm^3 \cdot min^{-1}$.
S3: solid-state exchange at 900 K for 10 h, nitrogen flow rate 70 $cm^3 \cdot min^{-1}$.
T: Tridymite phase.

graphs of the calcined MAPO-36 and Na exchanged MAPO-36 samples prepared from liquid and contact induced cation exchanges. The crystal size and shape of the sample prepared by Na exchange in liquid media are similar to the calcined MAPO-36. This indicates that the morphology is unaffected by liquid cation exchange and with subsequent heating at 773 K. In the case of the contact induced cation exchanged samples, the morphology is drastically affected. At lower solid-state exchange temperature (723 K), very few crystals with the thin rod-like shape (crystal shape similar to MAPO-36) were observed in NaMAPO-36[S1]. The original morphology of most of the crystals has been transformed from thin rod-like to irregular shaped aggregates. These irregular shaped aggregates are observed because of formation of tridymite phase. With increasing the solid-state exchange temperature (823 K and 900 K), more and more tridymite particles are formed. NaMAPO-36[S2] and NaMAPO-36[S3] show the presence of irregular shaped particles and dense phase.

The pore volume, external surface area and total surface area of the unmodified and modified MAPO-36 samples are presented in Table 1. The pore volume and total surface area of the NaMAPO-36[L] is decreased by 53% as compared with the MAPO-36. The decrease is expected because of the partial blockage of the channels in MAPO-36 by Na^+ cations. The

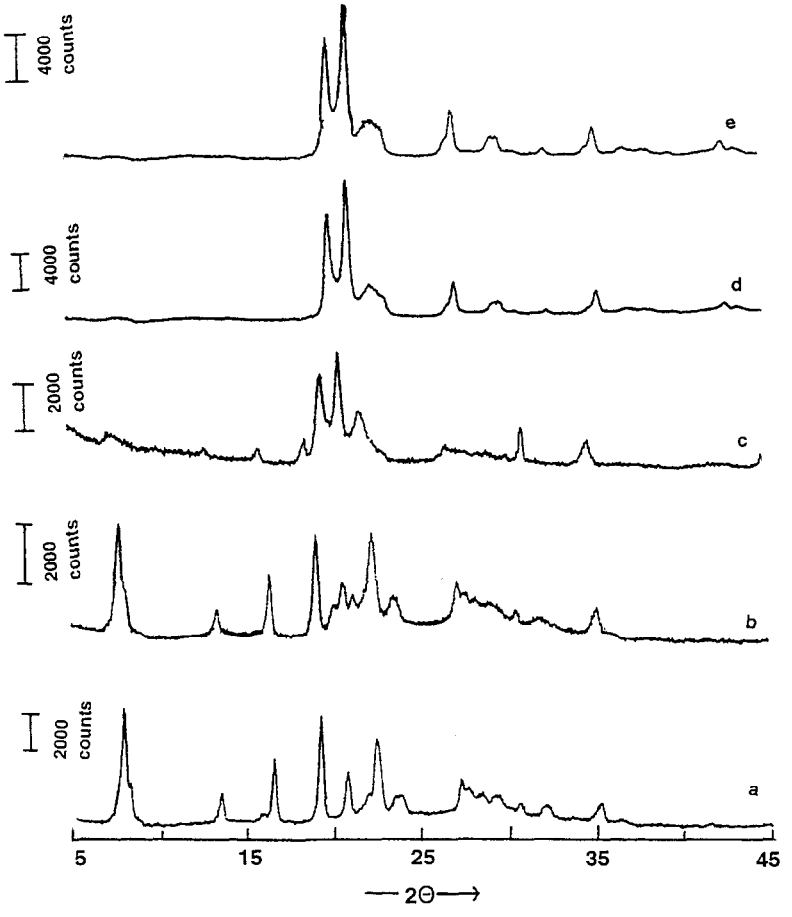

Fig. 1. X-ray powder diffraction patterns of the (a) MAPO-36, (b) NaMAPO-36[L], (c) NaMAPO-36[S1], (d) NaMAPO-36[S2] and (e) NaMAPO-36[S3].

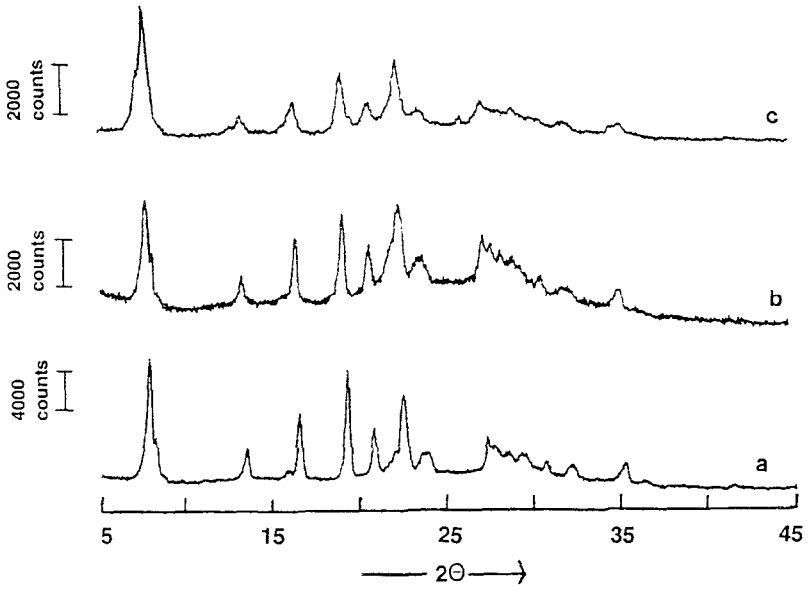

Fig. 2. X-ray powder diffraction patterns of the (a) MAPO-36, (b) Cs-MAPO-36[L] and (c) CaMAPO-36[L].

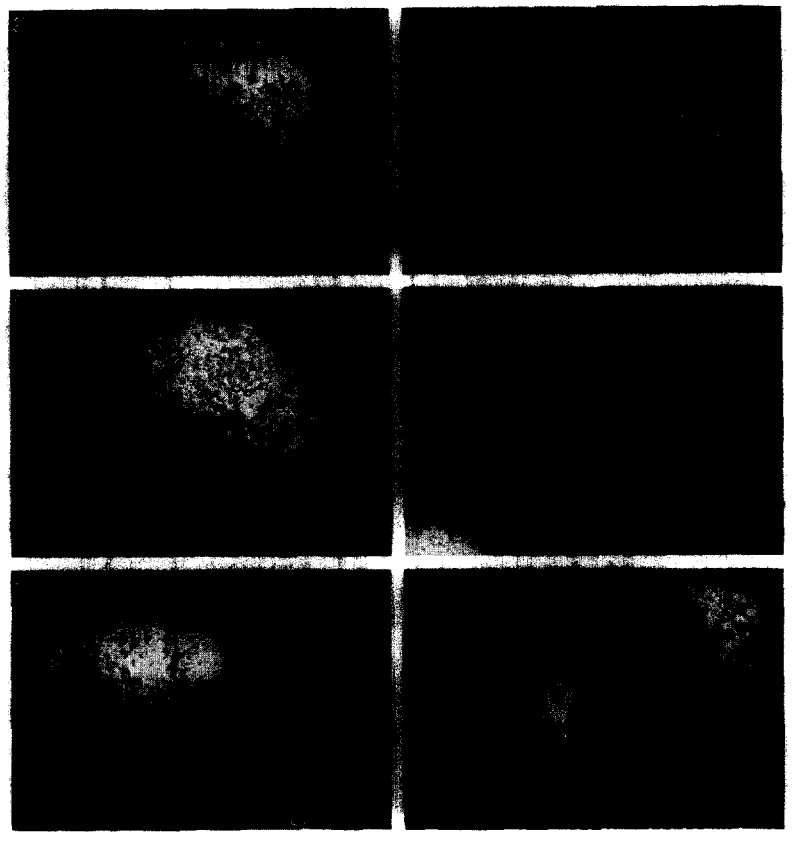

Fig. 3. Scanning electron photograph of the (a) calcined MAPO-36 (b) NaMAPO-36[L], (c) NaMAPO-36[S1], (d) NaMAPO-36[S2] and (e) NaMAPO-36[S3].

NaMAPO-36 samples prepared by solid-state cation exchange method at different temperatures exhibits sudden reduction in pore volume, external surface areas and total surface areas. Only the NaMAPO-36[S1] sample prepared at 723 K possess 4.6% of micropore volume and 6% of the total surface area as compared with that of parent MeAPO. The NaMAPO-36[S2] and NaMAPO-36[S3] samples prepared at higher temperatures (823 and 900 K) do not indicate microporous nature. The behaviour of samples in the sorption of water was investigated using the thermogravimetric balance. The samples were saturated by water vapour at 303 K for more than 20 h. The amount of water sorbed in the MAPO-36, NaMAPO-36[L], NaMAPO-36[S1], NaMAPO-36[S2] and NaMAPO-36[S3] was 23.5 [1], 14.1 [0.6], 9.2 [0.4], 1.5 [0.06] and 0.5 [0.02] wt.-%, respectively. The relative ratio of water sorbed in the samples with respect to the MAPO-36 is given in the square brackets. The lower amount of water sorbed by the NaMAPO-36[S1-S3] samples is due to the transformation of the ATS phase (microporous) to the dense tridymite phase.

Fig. 4 shows FTIR spectra of the MAPO-36 and sodium exchanged MAPO-36 samples. The IR spectrum of Na MAPO-36[L] is similar to that of MAPO-36 indicating the ATS phase is unaffected after the Na exchange in liquid aqueous media. A striking difference in the lattice vibration region is observed when the Na exchange is carried out in the solid-state at different temperatures. In the MAPO-36 and NaMAPO-36[L], the bands between 1200 and 1000, 720, 653 and 480 cm^{-1} are assigned to asymmetric stretch of TO_4 tetrahedra, symmetric stretch, vibration in double ring region and to TO-bend, respectively. These bands are shifted to higher frequencies in the NaMAPO-36[S1], NaMAPO-36[S2] and NaMAPO-36[S3] with the solid-state treatment temperature. The IR spectra show the formation of tridymite phase in the NaMAPO-36[S1], NaMAPO-36[S2] and NaMAPO-36[S3] samples. The formation of tridymite phase increases in these samples with

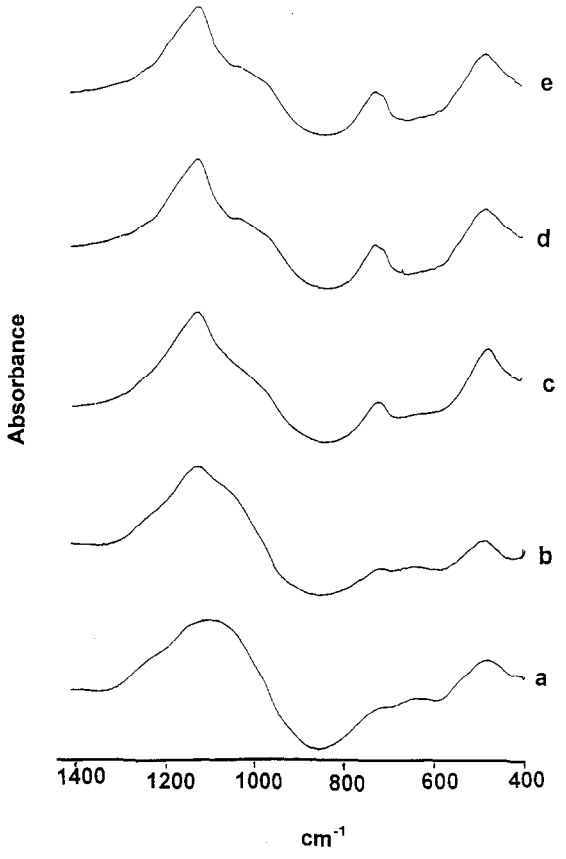

Fig. 4. FTIR spectra of (a) calcined MAPO-36 (b) Na-MAPO-36[L], (c) NaMAPO-36[S1], (d) NaMAPO-36[S2] and (e) NaMAPO-36[S3].

the solid-state treatment temperature. The IR spectrum of the tridymite phase show major bands at 1129, 1035, 730, 486 cm^{-1} and particularly, increase in area of the band at 730 cm^{-1} is observed in the sample NaMAPO-36[S1] to NaMAPO-36[S3].

Fig. 5 shows the ^{27}Al MAS NMR spectra of the MAPO-36 and Na exchanged MAPO-36 samples. The assignments of the ^{27}Al chemical shifts to tetrahedrally and higher coordinated Al are given in Table 2. In the MAPO-36 and NaMAPO-36[L, S1-S3] samples, the ^{27}Al chemical shifts (range 41.75–41.9 ppm) of the tetrahedrally coordinated Al is not significantly altered. However, in the case of contact induced cation exchanged samples {NaMAPO-36[S1–S3]}, the peak becomes more symmetric and

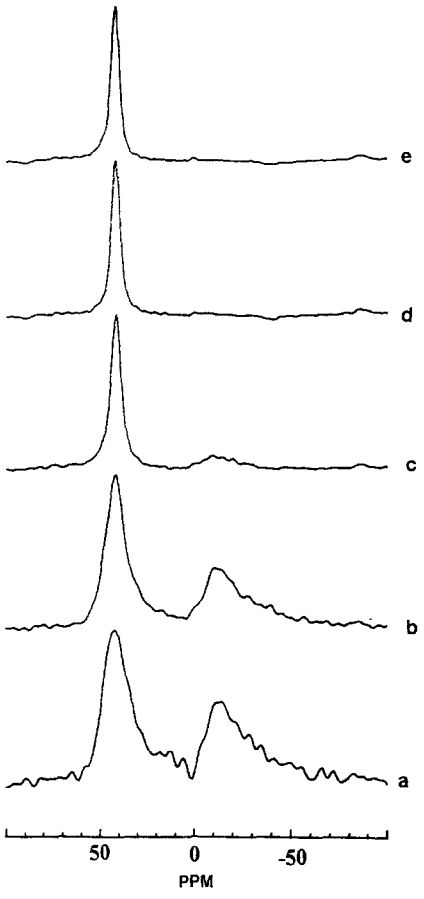

Fig. 5. ^{27}Al MAS NMR of the (a) calcined MAPO-36 (b) NaMAPO-36[L], (c) NaMAPO-36[S1], (d) NaMAPO-36[S2] and (e) NaMAPO-36[S3].

narrow with the increase in temperature. The second ^{27}Al peak observed (range −9.5 to −11.5 ppm) in the MAPO-36, NaMAPO-36 and NaMAPO-36[S1] is due to the five fold coordinated Al. The absence five coordinated Al peak and the increased symmetriness of the tetrahedral Al peak in the NaMAPO-36[S2] and NaMAPO-36[S3] indicated the complete conversion of the microporous phase to dense phase. The Al coordination is unaffected when the cation exchange is carried out in the liquid medium whilst it is strongly affected during solid-state cation exchange process, particularly above 723 K. The ^{27}Al MAS NMR spectra for the CsMAPO-36[L] and CaMAPO-36[L] molecular sieves presented in Fig. 6 (Table 2) show no changes in Al coordination. Only higher the ^{27}Al chemical shifts (tetrahedral Al) is observed in the CaMAPO-36[L] as compared with the MAPO-36.

Figs. 7 and 8 show the cross polarisation and high power decoupling spectra of the MAPO-36 and sodium exchanged samples. The ^{31}P NMR chemical shifts of the MAPO-36 samples are presented in Table 2. In the MAPO-36,

Table 2
Assignment of the ^{27}Al and ^{31}P NMR chemical shifts of the ATS aluminophosphate samples

Material	^{27}Al NMR (ppm)		^{31}P NMR (ppm)		
	Tetrahedral Al	Al [a]	I	II	III
MAPO-36	41.9	−11.6	−23.9	−14.5	
NaMAPO-36[L]	41.9	−11.1	−24.0	−14.5	
NaMAPO-36[S1]	41.8	−9.5	−29.8	−14.5	
NaMAPO-36[S2]	41.75	–	−29.1	−9.3	−3.06
NaMAPO-36[S3]	41.8	–	−29.7	−8.84	−1.45
CsMAPO-36[L]	41.9	−11.6	–	–	
CaMAPO-36[L]	43.3	−11.5	−24.6	−14.0	

[a] Five-fold coordinated Al.

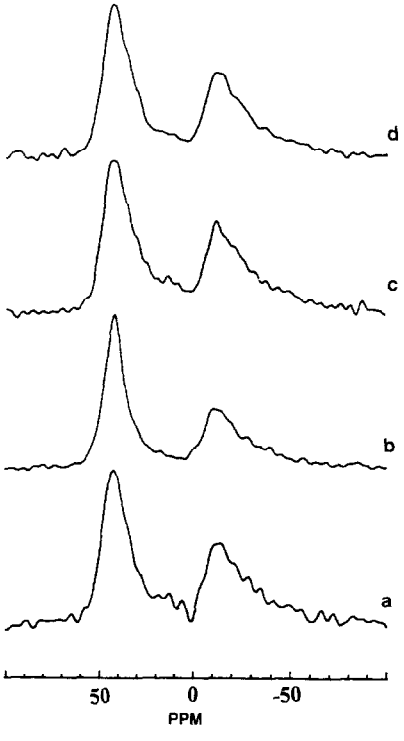

Fig. 6. ^{27}Al MAS NMR of the (a) calcined MAPO-36 (b) NaMAPO-36[L], (c) CsMAPO- 36[S1] and (d) CaMAPO-36[L].

NaMAPO-36[L] and CaMAPO-36[L] samples, where the structure is intact, the ^{31}P NMR peaks I and II are assigned to P(4 Al) and P(3 Al, 1 Mg), respectively. The peaks are assigned according to the assignments reported by previous authors [14,15]. The as-synthesised MAPO-36 [14] shows a line shape different from that of the ^{31}P NMR peaks from those of calcined MAPO-36, and the samples prepared by the liquid cation-exchange method (NaMAPO-36[L], CaMAPO-36[L]). In the calcined and liquid mediated cation exchange samples, the peaks are more broadened and ^{31}P NMR resonances are less resolved indicating distortion of the aluminophosphate framework. The ^{31}P NMR chemical shift is also affected by the changes in the coordination of some of the Al (tetrahedral to octahedral) due to the presence of water molecules in the channels. The line shape of similar ^{31}P NMR peaks observed in the calcined MAPO-36 (Fig. 7 and Fig. 8a), NaMAPO-36[L] (Fig. 7b and Fig. 8b) and CaMAPO-36[L] (Fig. 7f and Fig. 8) samples [obtained with CP (Fig. 7) and HPDEC (Fig. 8)] indicated the structure and chemical environment of the MAPO-36 are least affected by the liquid cation exchange method. Comparison of the ^{31}P NMR spectra measured with cross polarisation (Fig. 7a,b,f) and with high power decoupling (Fig. 8a,b,f)

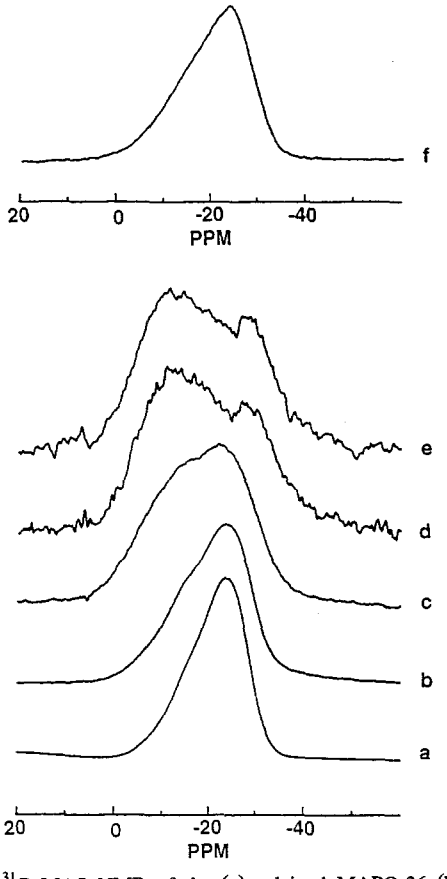

Fig. 7. ^{31}P MAS NMR of the (a) calcined MAPO-36 (b) NaMAPO-36[L], (c) NaMAPO- 36[S1], (d) NaMAPO-36[S2], (e) NaMAPO-36[S3] and (f) CaMAPO-36[L] samples with cross polarization.

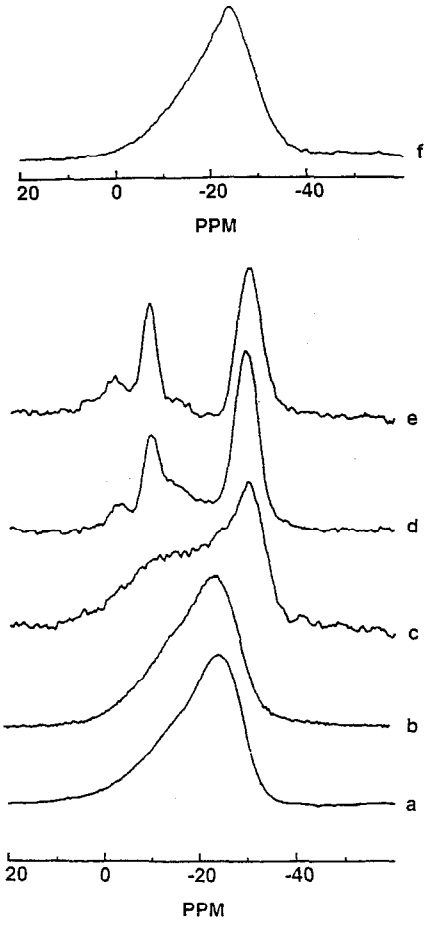

Fig. 8. ^{31}P MAS NMR of the (a) calcined MAPO-36 (b) NaMAPO-36[L], (c) NaMAPO- 36[S1], (d) NaMAPO-36[S2], (e) NaMAPO-36[S3] and (f) CaMAPO-36[L] samples with high-power decoupling.

reveals absence of extraneous POH group in MAPO-36, NaMAPO-36[L] and CaMAPO-36[L].

The ^{31}P NMR spectra (Fig. 7 and Fig. 8c,d,e) of the NaMAPO-36[S1–S3] samples prepared by the contact-induced cation exchange method are significantly different from those of calcined MAPO-36, NaMAPO-36[L] and CaMAPO-36[L]. The possible cause of different line shapes and additional peaks in the ^{31}P spectra of the contact induced cation exchange samples prepared at different temperatures is the phase transformation during the solid-state reaction. After partial or complete phase conversion or structural collapse of the MAPO-36, the formation of $AlPO_4$, MgO, $MgPO_4$ or other mixed phases are expected. Comparison of the ^{31}P NMR spectra of solid-state samples [NaMAPO-36 (S1–S3)] measured with [Fig. 7c,d,e] and without (Fig. 8c,d,e) ^{1}H cross polarisation reveals that POH group make significant contribution to the spectra. The presence of POH groups (as defects) is associated with the transformed phase (i.e. new phase formed after the solid-state reaction). The ^{31}P NMR chemical shifts of these samples are different from those of MAPO-36, NaMAPO-36[L] and CaMAPO-36[L] samples. The ^{31}P NMR chemical shift of peak II of NaMAPO-36[S1] sample is similar to that of MAPO-36. NaMAPO-36[S1] possesses tridymite as a major phase and ATS as minor phase. With the increase in the treatment temperature, the ^{31}P chemical shift of peak II in NaMAPO-36[S2,S3] samples increases (i.e. become less negative). The observed chemical shift of ^{31}P (HPDEC) in the $MgPO_4$ is -7.6 ppm. Considering the closeness of the ^{31}P chemical shift in $MgPO_4$ with that of NaMAPO-36[S3], the possibility of the presence of $MgPO_4$ phase in a small extent cannot be neglected.

In Table 3, the results of *o*-xylene conversion over MAPO-36 are compared with similar results obtained with NaMAPO-36[L], NaMAPO-36[S1–S3]. MAPO-36 showed higher conversion and concentration of toluene and C_9^+-aromatics than NaMAPO-36[L], NaMAPO-36[S1–S3] samples which is due to the presence of strong acid sites on MAPO-36. In NaMAPO-36[L], the activity is reduced because of the replacement of protons by sodium cations. The lower conversion of *o*-xylene over NaMPO-36[L] is due to the decrease in the acidity and partial blockage of channels by sodium cations. NaMAPO-36[L] shows higher *p*-xylene selectivity as compared with MAPO-36. The presence of Na in the channels of MAPO-36 increases diffusional resistance which in turn affects the *p*-xylene/*m*-xylene ratio.

The *o*-xylene conversion over the samples prepared by solid-state cation exchange is much lower. The *o*-xylene conversion over the samples decreases with the increase in the solid-state reaction temperature. The lower *o*-xylene conversion over these materials is because of the

Table 3
Comparison of the catalytic activity of the MAPO-36, NaMAPO-36[L], NaMAPO-36[S1], NaMAPO-36[S2] and NaMAPO-36[S3] samples in the *o*-xylene conversion reaction

Material	Conversion (%)	Product distribution (wt.-%)								*p*-Xylene/*m*-xylene	Xylene loss (%)
		Aliphatics	Benzene	Toluene	*p*-Xylene	*m*-Xylene	*o*-Xylene	C_{9+}-aromatics	Total		
MAPO-36	56.7	0.3	0.4	4.8	18.2	25.6	43.3	7.4	100	0.71	12.9
NaMAPO-36[L]	14.2	0.3	0.3	1.4	5.4	6.4	85.8	0.4	100	0.84	2.4
NaMAPO-36[S1]	3.4	0.2	0.2	0.2	1.1	1.6	96.6	0.1	100	0.68	0.7
NaMAPO-36[S2]	1.3	0.1	0.1	0.1	0.3	0.6	98.7	–	100	0.50	0.4
NAMAPO-36[S3]	0.9	0.1	0.1	0.1	0.2	0.4	99.1	–	100	0.50	0.3

Reaction conditions: catalyst weight: 50 mg; nitrogen flow rate: 125 $cm^3 \cdot min^{-1}$; pulse size 5 μl; temperature 673 K.

partial/complete transformation of the active catalyst (ATS) phase to less active phase (tridymite). The acidity and microporous nature of the MAPO-36 catalyst are strongly affected during the solid-state reaction in the presence of alkali chloride (NaCl) at different temperatures (723–900 K). It seems that the alkali metal salts influences the stability of the metal aluminophosphate materials. Similar observation related to the stability of the aluminophosphate molecular sieves in the presence of inorganic salts was reported by Wilson [16]. The presence of high concentrations of alkali metal or ammonium salts soluble in water in AlPO synthesis mixture interfere with nucleation or reduces the stability of the final product.

4. Conclusions

On basis of the above investigation results it is concluded that: (i) the MAPO-36 materials can be easily cation exchanged in liquid media without having any negative impact on the crystal structure, (ii) MAPO-36 tends to lose its crystal structure/ATS phase when the cation exchange samples are prepared by the contact-induced cation exchange method using alkali metal chloride, (iii) complete ATS phase transformation to tridymite takes place during solid-state reaction at 823 K, (iv) as compared with zeolites (X, ZSM-5, etc.), the metal aluminophosphate framework is not stable in the presence of sodium chloride at high temperatures. The presence of sodium chloride have detrimental effect on the MAPO-36 structure.

Acknowledgements

We thank Dr. Jim Hook, UNSW NMR Facility for assistance with the NMR measurements. The authors are sincerely thankful to Prof. R.F. Howe, School of Chemistry, The University of New South Wales, Sydney, Australia, for providing the experimental facilities and helpful discussions.

References

[1] E.M. Flanigen, B.M. Lok, R.L. Patton and S.T. Wilson, Pure Appl. Chem. 58 (1986) 1351 .
[2] S.T. Wilson and E.M. Flanigen, ACS Symp. Ser. 398 (1988) 329.
[3] D.B. Akolekar, J. Catal. 144 (1993) 148.
[4] D.B. Akolekar, J. Chem. Soc., Faraday Trans. 90 (7) (1994) 1041.
[5] J.A. Rabo, in: ed. J.A. Rabo, Salt Occlusion in Zeolite Crystals in Zeolite Chemistry and Catalysis, ACS Symp. Ser. 171 (Am. Chem. Soc., Washington, D.C., USA, 1976) pp. 332–349.
[6] J.A. Rabo and P.H. Kasai, Progress in Solid-State Chemistry (Pergamon, Oxford, 1975) pp. 1–19.
[7] A. Clearfield, C.H. Saldarriaga and R.C. Buckley, in: ed. J.B. Uytterhoeven, Proceedings of the 3rd International Conference on Molecular Sieves, Zürich, September 3–7, 1973, Recent Progress Reports, Paper No. 130 (University of Leuwen Press, Leuwen, Belgium) pp. 241–245.
[8] H. Beyer, P.A. Jacobs and J.B. Uytterhoeven, J. Chem. Soc., Faraday Trans. 72 (1976) 674.
[9] A.V. Kucherov and A.A. Slinkin, Zeolites 6 (1986) 175.
[10] H.K. Beyer, G. Borbely and H.G. Karge, Zeolites 8 (1988) 79.
[11] G. Borbely, H.K. Beyer, L. Radics, P. Sandor and H.G. Karge, Zeolites 89 (1989) 428.
[12] D.B. Akolekar, J. Catal. 143 (1993) 227.
[13] V.S. Nayak and V.R. Choudhary, Appl. Catal. 4 (1982) 333.
[14] D.B. Akolekar and R.F. Howe, J.Chem. Soc., Faraday Trans. (1997) submitted for publication.
[15] P.J. Barrie and J. Klinowski, J. Phys. Chem. 93 (1989) 5972.
[16] S.T. Wilson, Stud. Surf. Sci. Catal. 58 (1991) 137.